JJMIE

Volume 2, Number 1, Mar. 2008
ISSN 1995-6665
Pages 23 - 30

Jordan Journal of Mechanical and Industrial Engineering

Novel Thermal Resistance Network Analysis of Heat Sink with Embedded Heat Pipes

Jung-Chang Wang *

Taiwan Microloops Corporation, Taoyuan, Taiwan

Abstract

This article utilizes the experimental method to investigate the thermal performance of heat sinks with one and two pairs of embedded heat pipes. A heat sink with embedded heat pipes transfers the total heat capacity from the heat source to both the base plate and heat pipes, and then disperses heat into the surrounding air via the forced convection. The heat transference from base plate to fins can be conducted through the examined results of the heat sink with and without the function of heat pipes. The heat capacity from heat pipes to fins is equal to the total heat minus the heat from base plate to fins. Therefore, the heat carried by embedded heat pipes can be found using the thermal resistance analytical approach stated in this article. The results show that two and four heat pipes embedded in the base plate carry 36% and 48% of the total dissipated heat respectively; in addition, when the total heating power of the heat sink with two embedded heat pipes is 140W, the total thermal resistance reaches its minimum value of 0.27ºC/W, while for the heat sink with four embedded heat pipes, when the total heating power is between 40W and 240W, the total thermal resistance is 0.24ºC/W, meaning that the thermal performance is better than that of heat sink with two embedded heat pipes.

Keywords: Thermal Resistance; embedded heat pipes;

Nomenclature

h	heat transfer coefficient, W/m^2.K
H	length from base plate to condensation section of heat pipes, m
H_1	length from base plate to adiabatic line, m
H_2	length from adiabatic line to condensation section of heat pipes, m
k	thermal conductivity, W/ m.K
Q	total heat transfer rate, W
Q_b^i	heat transfer rate from base plate to fins, W
Q_j^i	heat transfer rate from j_{th} position heat pipes to fins, W
R	thermal resistance, K/W
R_t^i	total thermal resistance, K/W
R_c^i	thermal contact resistance, K/W
R_n^i	fin-base convective thermal resistance, K/W
R_{hj}^i	base to j_{th} position heat pipes thermal resistance, K/W
R_{pj}^i	j_{th} position heat pipes thermal resistance, K/W
R_{fj}^i	j_{th} position fin-pipe convective thermal resistance, K/W
T	temperature, K
T_b	one-dimensional temperature of adiabatic line, K
T_{cj}^i	mean temperature of condensation section of heat pipes, K
T_{ej}^i	mean temperature of evaporation section of heat pipes, K
T_u^i	mean upper surface temperature of base plate, K

Subscripts

a	ambient
b	base plate
d	lower central surface of base plate
f	fin
h	heat source
j	position of embedded heat pipes

Superscript

i	the sum of embedded heat pipes

* Corresponding author. e-mail: jc_wang@microloops.com

1. Introduction

Since 1971, when the Intel Corporation launched the first chip (with 10μm wires and 2300 transistors) , the number of transistors in a chip has increased to over ten million. This means that an equivalent surface area of chip produces far greater heat than previously, leading to an increase in critical heat flux speed. The maximum limited temperature that can be borne by silicon chip in electronic components is 120ºC, with a normal operating temperature of under 70ºC. The reliability of electronic components drops by 10% for each increase of 2ºC in normal operating temperature[1], and high temperature is a major reason for the malfunctioning or shortening of life of electronic components. Thus, it is necessary to quickly remove high heat generated by electronic components for a normal operating temperature of under 70ºC.

In the past, the method used for solving the high heat capacity of electronic components has been to install a heat sink with a fan directly on the heat source, removing the heat through forced convection. Webb[2] pointed out that it is necessary to increase the fin surface and fan speed of the direct heat removal heat sink in order to solve the ever-increasing high heat flux generated by CPUs. The total thermal resistance is used to evaluate the thermal performance of a heat sink. Duan and Muzychka[3] increased the heat dispersing surface area of the heat sink fins, reducing the total thermal resistance from 0.55 ^{o}C/W to 0.35 ^{o}C/W. Lin et al.[4] boosted the fan speed to obtain an optimum total thermal resistance value of 0.33 ^{o}C/W at a maximum speed of 4000rpm. However, increasing the surface area results in an increase in cost and boosting the fan speed results in noise, vibration and more power consumption, which increase the probability of failure to electronic components.

In a heat sink with embedded heat pipes, the use of heat pipes to rapidly transfer heat from the heat source to the fins, without increasing the surface area of the fins or increasing the speed of the fan, makes it possible to reduce the total thermal resistance to under 0.3ºC/W. Due to high thermal conductivity of the heat pipes, the thermal resistance is very low at about $10^{-1} \sim 10^{-3}$ ^{o}C/W[5-7]. Xie et al.[8] conducted an experiment combining a 4mm diameter heat pipe and a heat sink, achieving an optimum total thermal resistance of 0.29 ^{o}C/W. Legierski and Wiecek [9] pointed out that the thermal performance of the heat sink with embedded heat pipes is better than that of an ordinary heat sink, with an optimum total thermal resistance value of 0.25 ^{o}C/W. Gernert et al.[10] used a heat sink with embedded heat pipes composed of a 25.4mm diameter heat pipe and an aluminum heat sink; when the maximum heat flux was 285W/cm^2, the minimum total thermal resistance value was 0.225ºC/W. Wang et al.[11] examined two horizontal embedded heat pipes of diameter 6mm inserted into base plate and fins in order to take heat capacity from heat source. From the results, the ratio of total heat capacity of embedded heat pipes is 36%. Therefore, a heat sink with embedded heat pipes is one of the best solutions for thermal problems of high heat generation in electronic components.

The heat sink with one and two pairs of embedded heat pipes studied in this article is shown in Fig.1(a) and Fig.1(b), respectively. The dimensions of the heat sink are 75 x 70 x 43 mm^3. The ends of heat pipes are inserted into the base plate as the evaporation section, and the other ends are embedded into the fins as the condensation section. Because the heat pipes are embedded into the left and right sides of the base plate in a parallel manner, and the heat source is placed directly onto the center of the base plate; therefore, the heat pipes bear equal heat from the heat source. Previous research only measures the contact, base plate and total thermal resistances of a heat sink with embedded heat pipes, without addressing the proportion of the total heat carried away via the heat pipes. In light of this, this study utilized experimental methods incorporating superposition method to calculate the heat carried to the fins through the base plate and embedded heat pipes, in order to find the ratio of total heat transferred through the heat pipes. These individual thermal resistances of contact, base plate, base to heat pipes, heat pipes, fins and the total thermal resistance can be obtained through thermal resistance analysis.

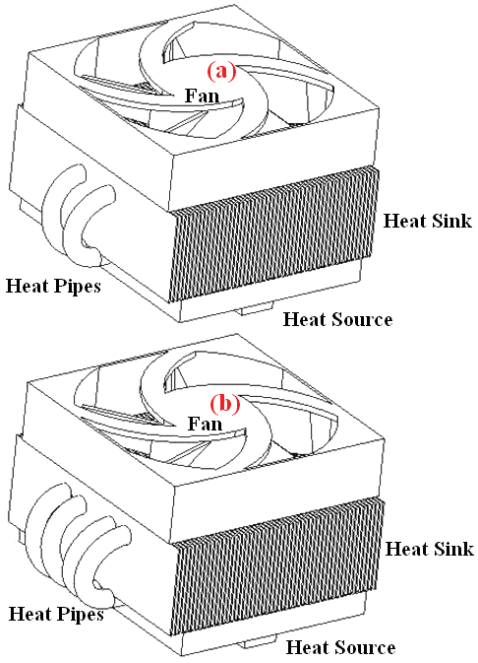

Figure 1: (a) Heat sink with one pair of embedded heat pipes, (b) Heat sink with two pairs of embedded heat pipes

2. Thermal Resistance Network

This paper use the superposition method for the heat sink with embedded heat pipes as shown in Fig. 2. The symbols i and j respectively denote the number and position of the embedded heat pipes. The total heating power Q is transferred from the heat source to the base plate and the heat pipes. The heating power Q_b^i is borne away by the base plate; the heat pipes are the adiabatic boundary conditions, and Q_b^i is transferred upward to the fins.

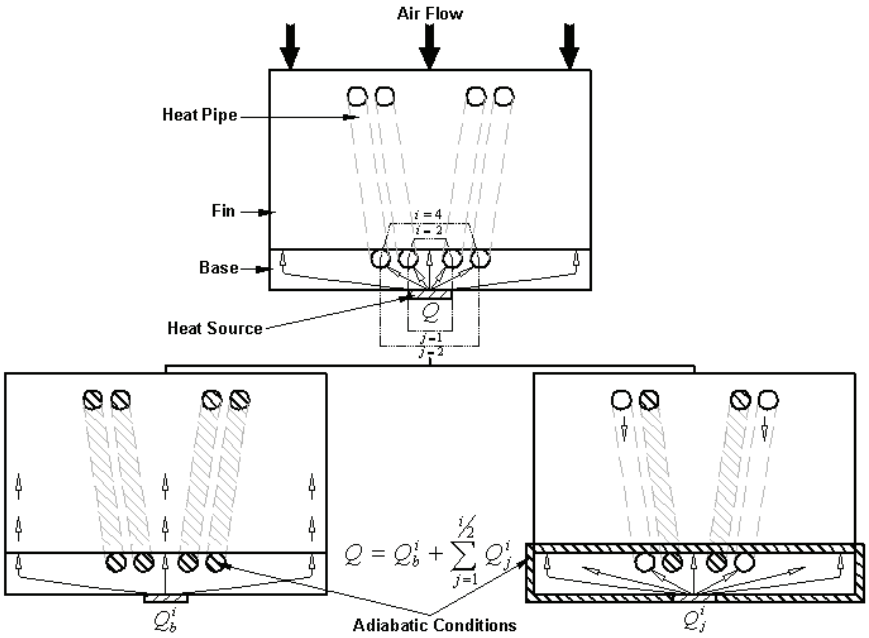

Figure 2: Superposition method of heat sink with embedded heat pipes

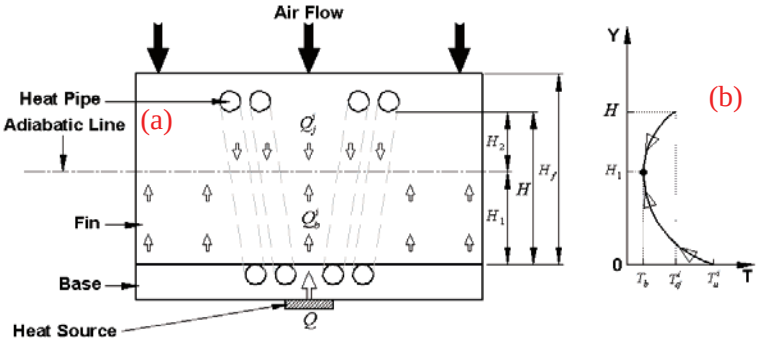

Figure 3: (a) Heat sink with embedded heat pipes heat flow pathways, (b) Fin temperature distribution

The heating power Q_j^i is carried away through the heat pipes laid in a parallel fashion to the left and right of the heat source; the base plate is the adiabatic boundary condition, and Q_j^i is transferred downward to the fins. Consequently, Q equals the sum of Q_b^i and Q_j^i from the superposition method. Because of measuring the thermal performance by separately testing the heat sink with and without the function of heat pipes, Q_b^i can be found from comparing the same temperature differences corresponding to the input heating power. Then Q_j^i equals to Q minus Q_b^i.

Assuming that Q_b^i and Q_j^i transfer heat as one-dimension steady heat flow model, and Q is divided into two pathways transferring heat from Q_b^i upward and Q_j^i downward to the fins as shown in Fig. 3(a). The region where temperature gradient equals to zero appearing between these two heat transfer pathways is called adiabatic line. The fins in this adiabatic position will not have heat transfer. The distance from the upper surface of the base plate to the condensation section of the heat pipes is H, and those from the adiabatic position to the upper surface of the base plate and to the condensation section of the heat pipes are H_1 and H_2 respectively. Figure 3(b) shows temperature distribution graph for the surface of the fins, where T_b is adiabatic temperature, T_{cj}^i is the temperature of the condensation section of the heat pipes, and T_u^i is the temperature of the upper surface of the base plate. Assuming these temperatures are uniform both on the upper surface of the base plate and on the condensation section of the heat pipes, the steady one-dimensional energy balance equation for fins is[12]

$$\frac{d^2T^i}{dY^2} - m^2\left(T^i - T_a^i\right) = 0 \qquad (1)$$

and

$$m = \sqrt{\frac{2h}{k_j t_f}} \qquad (2)$$

where h represents the convective heat transfer coefficient, k_f is the fin conductivity , t_f is the fin thickness and T_a^i is the ambient temperature. The specified boundary conditions can be expressed as

$$T^i = T_u^i \ at\ Y = 0 \ \ and \ \ T^i = T_{cj}^i \ at\ Y = H \qquad (3)$$

The temperature profile for the fins can be obtained from Eq.(1) as

$$T^i(Y) = T_a^i + \left[\frac{(T_u^i - T_a^i)e^{mH}}{e^{mH} - e^{-mH}} - \frac{(T_{cj}^i - T_a^i)}{e^{mH} - e^{-mH}}\right]e^{-mY} + \left[\frac{(T_{cj}^i - T_a^i)}{e^{mH} - e^{-mH}} - \frac{(T_u^i - T_a^i)e^{-mH}}{e^{mH} - e^{-mH}}\right]e^{mY} \quad (4)$$

From the definition of adiabatic line,

$$\frac{\partial T^i}{\partial Y} = 0 \ \ at \ Y = H_1 \quad (5)$$

The location of adiabatic line can be shown as

$$H_1 = \frac{1}{2m}\ln\left[\frac{(T_u^i - T_a^i)e^{mH} - (T_{cj}^i - T_a^i)}{(T_{cj}^i - T_a^i) - (T_u^i - T_a^i)e^{-mH}}\right] \quad (6)$$

Figure 4 shows an analysis of the thermal resistance network of the heat sink with embedded heat pipes. When the superscript i equals 2 or 4, it represents, respectively, that the heat sink has a total of two or four embedded heat pipes. The heat sink with two embedded heat pipes has base plate thermal resistance R_b^2 and fin-base convective resistance R_n^2 in the Q_b^2 pathway, and base to heat pipes resistance R_{h1}^2, heat pipes resistance R_{p1}^2 and fin-pipe convective resistance R_{f1}^2 in the Q_1^2 pathway when i equals to 2. When i is 4, the heat sink with four embedded heat pipes has a base plate thermal resistance R_b^4, fin-base convective resistance R_n^4 in the Q_b^4 pathway, base to inner heat pipes resistance R_{h1}^4, inner heat pipes resistance R_{p1}^4, inner fin-pipe convective resistance R_{f1}^4, base to outer heat pipes resistance R_{h2}^4, outer heat pipes resistance R_{p2}^4 and outer fin-pipe resistance R_{f2}^4 in Q_1^4 and Q_2^4 pathway, respectively.

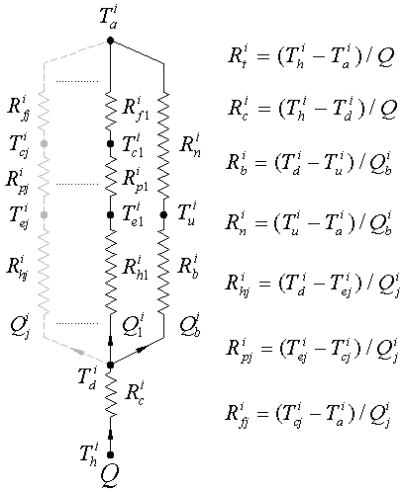

Figure 4: Thermal resistance analysis network

The total thermal resistance R_t^i can be expressed as the sum of the thermal contact resistance R_c^i and the thermal resistances on the pathways of Q_b^i and Q_j^i, which is

$$R_t^i = R_c^i + \frac{1}{\frac{1}{(R_b^i + R_n^i)} + \sum_{j=1}^{i/2}\frac{1}{(R_{hj}^i + R_{pj}^i + R_{fj}^i)}} \quad (7)$$

In Eq. (7), R_t^i is defined as the temperature difference (the temperature of heat source T_h^i minus the ambient temperature T_a^i) divided by total heating power Q. R_c^i is defined as the effective temperature difference at the interface (T_h^i minus the temperature at the center of the lower surface of the base plate T_d^i) divided by Q. R_b^i is defined as the temperature difference (T_d^i minus the average temperature at upper surface of the base plate T_u^i) divided by Q_b^i. R_n^i is defined as the temperature difference (T_u^i minus T_a^i) divided by Q_b^i. R_{hj}^i is defined as the temperature difference (T_d^i minus the temperature of evaporation section of heat pipes T_{ej}^i) divided by Q_j^i. R_{pj}^i is defined as the temperature difference (T_{ej}^i minus the temperature of condensation section of heat pipes T_{cj}^i) divided by Q_j^i. R_{fj}^i is defined as the temperature difference (T_{cj}^i minus T_a^i) divided by Q_j^i.

3. Experimental Investigation

The experimental methods stated in this paper are mainly aimed at testing the thermal performance of the heat sink with embedded heat pipes as shown in Fig. 5. The heat pipes are bending pipes with a diameter 6 mm and a total length 170 mm. The length of evaporation section and condensation section is 65 mm respectively, and the insulated length is 40 mm. The materials of heat pipe's container and wick type are copper metal and sintered structure of pure copper powder respectively. According to the superposition method for the heat sink with embedded heat pipes, the first step is to measure the entire thermal performance of the heat sink with embedded heat pipes, then measure that of the heat sink with losing the function of embedded heat pipes at positions where j is equal to $1,2\ldots i/2$, successively. The heat capacity transference from the base plate and the heat pipes to the fins can be obtained by comparing the individual results in the same temperature differences respectively.

The experimental test includes the experiments of heat sinks with two and four embedded heat pipes respectively. The upper surface of the dummy heater is coated with thermal grease to reduce contact resistance.

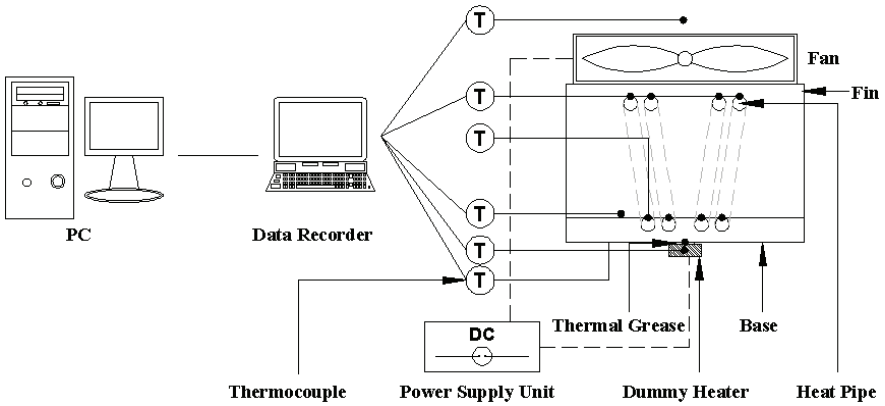

Figure 5**:** Experimental apparatus for Heat sink with embedded heat pipes

A T-type thermocouple is attached to the upper surface of the dummy heater to measure the temperature (T_h^i). Six thermocouples are attached to the center of the lower surface of base plate and five points along the diagonal of the upper surface of base plate, measuring the temperatures at the center of the lower surface of the base plate (T_d^i) and the average temperature of the upper surface of the base plate (T_u^i). Computational Fluid Dynamic commercial software (Icepak) is used to calculate the average temperature of T_u^i, which is compared with the experimental measurement of five-point average value and develops a correlation between them within an error of ±3%. A fan is placed on the top of heat sink to disperse heat through forced convection. A thermocouple is placed on the top of the fan to measure the ambient temperature (T_a^i). Thermocouples are attached to the evaporation and condensation sections of heat pipes to measure the temperatures of T_{ej}^i and T_{cj}^i. This experiment starts with a heating power of 40W and increases it up to 240W by increments of 20W.

After separately testing the full thermal performance of the above two experiments for the heat sink with function of embedded heat pipes, let all heat pipes in the heat sink with two embedded heat pipes fail to function ,and allow the inner (j = 1) and outer (j = 2) heat pipes in the heat sink with four embedded heat pipes to fail to function successively. The heat sink experiments without the function of heat pipes are then performed, and the corresponding thermal resistances can be determined.

The thermocouples used in the experiment have a measurement error of ± 0.5 ºC. The cooling circulator manufactured by Firstek Scientific Co., Ltd., has a measurement error of ± 0.5 ºC. The data recorder manufactured by Yokogawa Co., Ltd., has a measurement error of ±1 %. The power supply unit has a measurement error of ±0.5 %. The maximum error for the thermal resistance is within ±5 %.

4. Results and Discussions

Figure 6 shows the experimental results of thermal performance lines for a heat sink with and without the function of two embedded heat pipes. As the heating power is increasing, the temperature difference ($T_u^2 - T_a^2$) between the upper surface of the base plate and the surrounding air also increases whether with or without the function of two heat pipes. The slopes of these two lines represent the thermal resistances. Because the slope of the upper line is greater than that of the lower, the thermal resistance without function of heat pipes is greater than that with function of two heat pipes. It means that the temperature difference ($T_u^2 - T_a^2$) is higher without the function of two heat pipes than that with the function of two heat pipes.

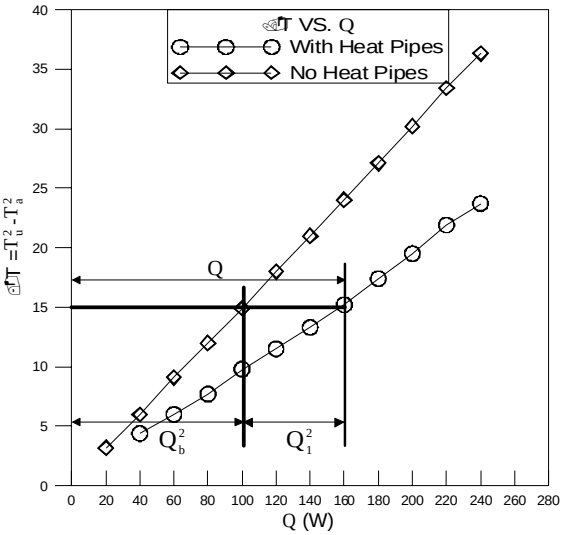

Figure 6**:** Performance curve for two embedded heat pipes under various heating power

This is because having an extra path transfers heat from heat pipes to surrounding and thus reduces the temperature difference. As the temperature difference for the two lines is fixed as shown in Fig.6, it reaches the thermal performance lines with two points at the power input with and without function of two heat pipes. The corresponding heating power represents the Q_b^2 in the heat sink without the function of two heat pipes and the total Q with the function of two heat pipes. The heat transfer rate Q_1^2 is equal to the total Q minus the Q_b^2. As indicated in Fig.6, the temperature difference is 15.2ºC, the heating power for Q is 160W, and the power for Q_b^2 is 102.6W. Therefore Q_1^2 equals 57.4W. Table 1 shows the ratio of bypass heating power to total heating power. The ratio (Q_b^2 / Q) is 64% and the ratio (Q_1^2 / Q) is 36%.

Table 1. Ratio of bypass heating power to total heating power of heat sink with two embedded heat pipes

Q (W)	Q_b^2/Q (%)	Q_b^2 (W)	Q_1^2/Q (%)	Q_1^2 (W)
40	67	26.9	33	13.1
60	67	40	33	20
80	64	51.4	36	28.6
100	65	65	35	35
120	63	76	37	44
140	63	88.6	37	51.4
160	64	102.6	36	57.4
180	64	116	36	64
200	65	129.5	35	70.5
220	66	146	34	74
240	66	157.4	34	82.6

Figure 7 shows the experimental results of thermal performance lines for a heat sink with and without the function of four embedded heat pipes. As is the case in Fig.6, the temperature difference of heat sink without function of embedded heat pipes is the same in the heat sink with embedded heat pipes, which is fixed the temperature difference of three curves in the Fig.7. The corresponding heat transference rate is equal to Q_b^4. Let the temperature difference of the inner embedded heat pipes be the same in the heat sink with four embedded heat pipes : Q_1^4 is equal to the corresponding heat transferring rate minus Q_b^4, and Q_2^4 is equal to Q minus Q_b^4 adding Q_1^4. As indicated in Fig.7, the temperature difference is 14.8ºC, the heating power for Q is 200W, the power for Q_b^4 is 104.4W, the power for Q_1^4 is 53.9W, and the power for Q_2^4 is 41.7W. Table 2 shows the ratio of bypass heating power to total heating power. The ratio (Q_b^4/Q) is 52%, the ratio (Q_1^4/Q) is 27%, and the ratio (Q_2^4/Q) is 21%.

Table 2. Ratio of bypass heating power to total heating power of heat sink with four embedded heat pipes

Q (W)	Q_b^4/Q (%)	Q_b^4 (W)	Q_1^4/Q (%)	Q_1^4 (W)	Q_2^4/Q (%)	Q_2^4 (W)
40	52	20.8	27	11	21	8.2
60	52	31.2	27	16.5	21	12.3
80	50	39.9	29	23.1	21	17
100	51	50.6	27	27.2	22	22.2
120	51	61.4	27	32.5	22	26.1
140	52	72.1	27	37.9	21	30
160	52	82.9	27	43.2	21	33.9
180	52	93.6	27	48.5	21	37.9
200	52	104.4	27	53.9	21	41.7
220	52	114.2	27	60.2	21	45.6
240	52	125.6	27	64.9	21	49.5

Figure 8 indicates the relationships of the base plate resistance R_b^i and the fin-base convective resistance R_n^i toward the heating power Q_b^i. These thermal resistance curves on the paths Q_b^i are a horizontal trend line as shown in Fig.8. R_b^2 and R_n^2 are approximately 0.25ºC/W and 0.15ºC/W respectively when Q_b^2 is between 26.9 and 157.4 W. R_b^4 and R_n^4 are approximately 0.28ºC/W and 0.14ºC/W respectively when Q_b^4 is between 20.8 and 125.6 W. They do not change as heating power increases. Thus, R_b^i and R_n^i in this experiment can be considered constants.

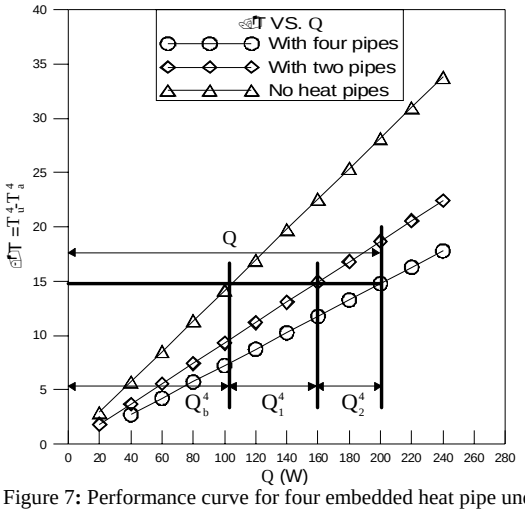

Figure 7**:** Performance curve for four embedded heat pipe under various heating power

The reason is that the components transferring heat through this path of heating power Q_b^i transferred from the base plate without function of heat pipes to the fins are all solid. The thermal physical properties of these components are the same when there is not much change in temperature. Thus R_b^i and R_n^i should remain constant. R_b^i and R_n^i obtained in this experiment are both constant, corroborating the correctness of the experimental results. The experimental results of R_b^4 is larger than that of R_b^2, resulting from the distortion effect of heat sink with four embedded heat pipes larger than that of heat sink with two embedded heat pipes. From above-mentioned experimental results, R_b^i increases and R_n^i decreases as i increases.

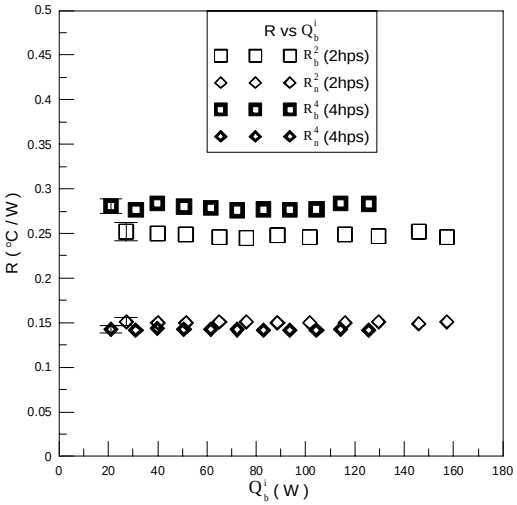

Figure 8**:** Relationships of base plate resistance R_b^i and fin-base convective resistance R_n^i with the heating power Q_b^i

Figure 9 indicates the base to heat pipes resistance R^i_{hj}, heat pipes resistance R^i_{pj} and fin-pipe convective resistance R^i_{fj} with heating power Q^i_j. R^2_{h1} drops from 0.43ºC/W to 0.33ºC/W under heating power of 13W to 40W. When Q^2_1 is 51.8W, it reaches a minimum value of 0.32ºC/W. R^2_{h1} rises from 0.33ºC/W to 0.39ºC/W under heating power of 57.6W to 82.6W. R^4_{h1} drops from 0.38ºC/W to 0.35ºC/W under heating power of 11W to 27.2W. When Q^4_1 is 37.9 W, it reaches a minimum value of 0.34ºC/W. R^4_{h1} rises from 0.36ºC/W to 0.41ºC/W under heating power of 43.2W to 64.9W. R^4_{h2} drops from 0.58ºC/W to 0.53ºC/W under heating power of 8.2W to 22.2W. When Q^4_2 is 30 W, it reaches a minimum value of 0.52ºC/W. R^4_{h2} rises from 0.58ºC/W to 0.61ºC/W under heating power of 37.8W to 49.6W.

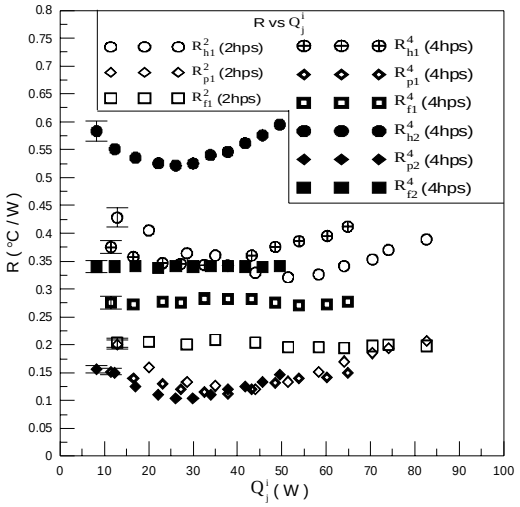

Figure 9: Relationships of the base to heat pipes resistance R^i_{hj}, heat pipes resistance R^i_{pj} and fin-pipe convective resistance R^i_{fj} with heating power Q^i_j

The fin-pipe convective resistance R^i_{fj} do not change much as the heating power increases, so they can be considered a constant in this experiment. When the Q^2_1 is 13W to 82.6W, R^2_{f1} is approximately 0.20ºC/W. R^4_{f1} is approximately 0.28ºC/W while Q^4_1 is 11W to 64.9W. R^4_{f2} is approximately 0.34ºC/W when the Q^4_2 is 8.2W to 49.6W. R^2_{p1} drops from 0.20ºC/W to 0.13ºC/W when Q^2_1 is between 13W and 44W. It reaches its minimum value of 0.12ºC/W when Q^2_1 is 51.8W. R^2_{p1} rises from 0.15ºC/W to 0.21ºC/W when Q^2_1 is between 57.6W and 82.6W. The R^4_{p1} drops from 0.15ºC/W to 0.12ºC/W when Q^4_1 is between 11W and 32.5W. It reaches its minimum value of 0.11ºC/W when Q^4_1 is 37.9W. The R^4_{p1} rises from 0.12ºC/W to 0.15ºC/W when Q^4_1 is between 43.2W and 64.9W. The R^4_{p2} drops from 0.16ºC/W to 0.11ºC/W when Q^4_2 is between 8.2W and 22.2W. It reaches its minimum value of 0.10ºC/W when Q^4_2 is 30W. The R^4_{p2} rises from 0.12ºC/W to 0.15ºC/W when Q^4_2 is between 37.8W and 49.6W. They change as the heating power changes.

Figure 10 shows the relationships of the total thermal resistance and thermal contact resistance to the total heating power Q. The contact thermal resistance is approximately 0.03ºC/W when the heating power is between 40W and 240W. Therefore the contact thermal resistance in this experiment can be seen as a constant. The total thermal resistance R^2_t drops from 0.32ºC/W to 0.27ºC/W when the heating power is between 40W to 140W and reaches its minimum of 0.27 ºC/W at 140W. R^2_t rises from 0.27ºC/W to 0.29ºC/W under 140W to 240W. This is because of the heating power increasing to the point that the embedded heat pipes are starting to function, and the total thermal resistance shows a decreasing trend. The heat pipes are unable to bear excessive higher heat at heating powers of above 240W, causing the evaporation section to produce more amounts of vapor than that of condensed liquid, resulting in the heat pipes losing performance, thereby increasing total thermal resistance. The total thermal resistance R^4_t is 0.24 ºC/W when the heating power is 40 to 240 W and does not change much as the heating power increases. This is because the four embedded heat pipes carry away 48% of the total heat, and the two outer heat pipes can share the load of the two inner heat pipes load, not causing R^4_t to increase.

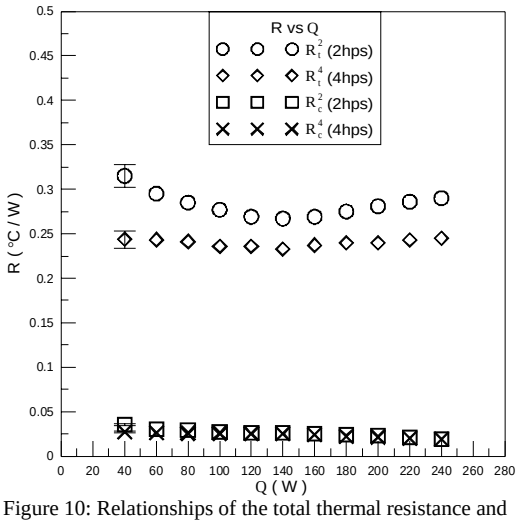

Figure 10: Relationships of the total thermal resistance and thermal contact resistance with heating power Q

Figure 11 indicates the temperature of heat source with total heat transference rate Q. The temperature of heat source T^i_h of heat sink with two (i = 2) and four (i = 4) embedded heat pipes can be calculated by Eq. (8) and Eq. (9) at heating power 40W to 240W respectively. When the T^i_h is 70ºC, the corresponding heating power Q of the heat sink with two and four embedded heat pipes is 131W and 164W individually. This means that the temperature of heat sink with four embedded heat pipes rises more slowly than that of two embedded heat pipes in the same heating power. The reason is that outer heat pipes of the heat sink with four

embedded heat pipes can bear and carry away an additional 33W of heat capacity from the heat source when the T_h^i is 70º. Furthermore, with respect to CPUs that emit high heat flux, a heat sink with four embedded heat pipes is able to carry away heat capacity faster than a heat sink with two embedded heat pipes, thereby attaining a lower CPU operating temperature.

$$T_h^2 = 0.30 \times Q + 30.6 \quad (8)$$

$$T_h^4 = 0.24 \times Q + 30.6 \quad (9)$$

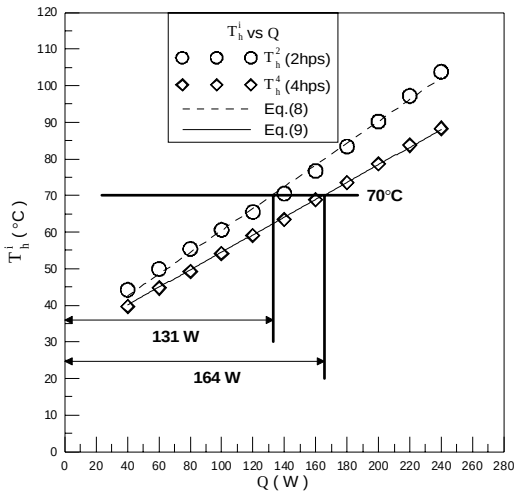

Figure 11**:** Relationships of the temperature of heat source with total heat transferring rate Q

5. Conclusions

Through these experiments in this study, it has been found that heat transfer rate Q_1^2 and Q_b^2 of heat sink with two embedded heat pipes occupy 36% and 64% of the total Q respectively, and Q_2^4, Q_1^4 and Q_b^4 of the heat sink with four embedded heat pipes account for 21%, 27% and 52% of the total Q individually. Moreover, the total thermal resistance of the heat sink with two embedded heat pipes is only affected by changes in the base to heat pipes thermal resistance and heat pipes thermal resistance over the heat flow path of the Q_1^2; that is, the total thermal resistance varies according to the functionality of the heat pipes. As for the total thermal resistance of heat sink with four embedded heat pipes, at 40W to 240W, the two outer heat pipes can carry away more heat, so the total thermal resistance is a constant. If the temperature of the heat source is not allowed to exceed 70º, the total heating powers of heat sink with two and four embedded heat pipes will not exceed 131W and 164W respectively. Finally, the superposition principal analytical method for the thermal performance of the heat sink with embedded heat pipes is completely established in the present paper.

References

[1] Bar-Cohen, A. D. Kraus, and S. F. Davidson, “Thermal frontiers in the design and packaging microelectronic equipment”. Mechanical Engineering, Vol. 105, No. 6, 1983, 53-59.

[2] Ralph L. Webb, “Next Generation Devices for Electronic Cooling with Heat Rejection to Air". ASME J. Heat Transfer, Vol.127, 2005, 2-10.

[3] Zhipeng Duan, and Yuri S. Muzychka, “Impingement air cooled plate fin heat sinks Part II- Thermal resistance model". IEEE Inter Society Conference on Thermal Phenomena, 2004.

[4] S. C. Lin, F. S. Chuang, and C. A. Chou, “Experimental study of the heat sink assembly with oblique straight fins". Experimental Thermal and Fluid Science, Vol. 29, 2005, 591–600.

[5] G.. P. Peterson. An introduction to heat pipe - modeling, testing, and applications. New York: John Wiley & Sons Inc.; 1994.

[6] Taxiong Wang, and G. P. Peterson, “Investigation of a Novel Flat Heat Pipe". ASME J. Heat Transfer, Vol. 127, 2005, 165-170.

[7] Faghri, Heat Pipe Science and Technology, Taylor and Francis Ltd., 1995.

[8] H. Xie, A. Ali, and R. Bhatia, “The use of heat pipes in personal computers". Inter Society Conference on Thermal Phenomena, 1998.

[9] Jaroslaw Legierski, and Boguslaw Wiecek, “Steady state analysis of cooling electronic circuits using heat pipes". IEEE Transactions on Components and Packing Technologies, Vol.24, No.4, 2001, 549-553.

[10] N. J. Gernert, J. Toth, and J. Hartenstine, “100 W/cm^2 and higher heat flux dissipation using heat pipes”. 13th International Heat Pipe Conference, 2004.

[11] J.C. Wang, H.S. Huang, and S.L. Chen, “Experimental investigations of thermal resistance of a heat sink with horizontal embedded heat pipes". International Communications in Heat and Mass Transfer, Vol. 34, 2007, 958-970.

[12] W. M. Rohsenow, J. P. Hartnett, and Y. I. Cho. Handbook of heat transfer .3 rd ed. McGraw-Hill; 1998.